

Structural characterization of a magnesium transporter of the SLC11/NRAMP family

Karthik Ramanadane, Monique S. Straub, Raimund Dutzler* and Cristina Manatschal*

Department of Biochemistry, University of Zurich, Zurich, Switzerland
(* corresponding author)

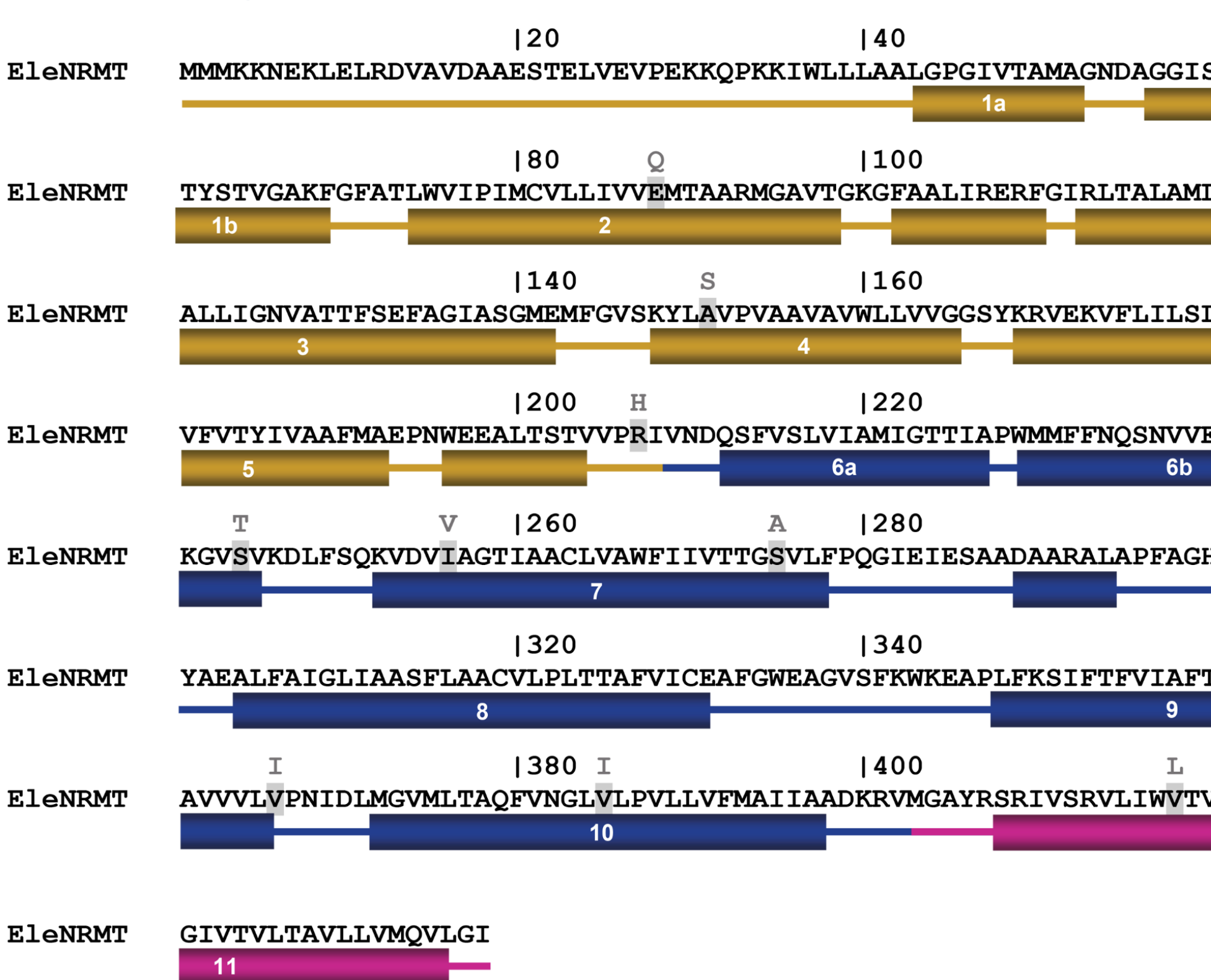
ABSTRACT

Divalent metal transporters (DMTs) of the **SLC11/NRAMP** family are proton coupled divalent transition metal symporters and are evolutionary highly conserved. Our previous structure of the transporter of *Staphylococcus capitis* (ScaDMT)¹ has revealed conserved residues that coordinate the transition metal ion. Extensive sequence alignments show that evolutionary distant DMT homologues comprise divergent residues at this site. Those transporters have been proposed to function as **NRAMP related Mg²⁺ transporters (NRMTs)** in bacteria^{2,3}. We selected EleNRMT as a promising candidate for biochemical characterization and proved that **EleNRMT is a non proton coupled Mg²⁺ transporter**³. However, structural informations to explain the basis of this substrate selectivity were lacking.

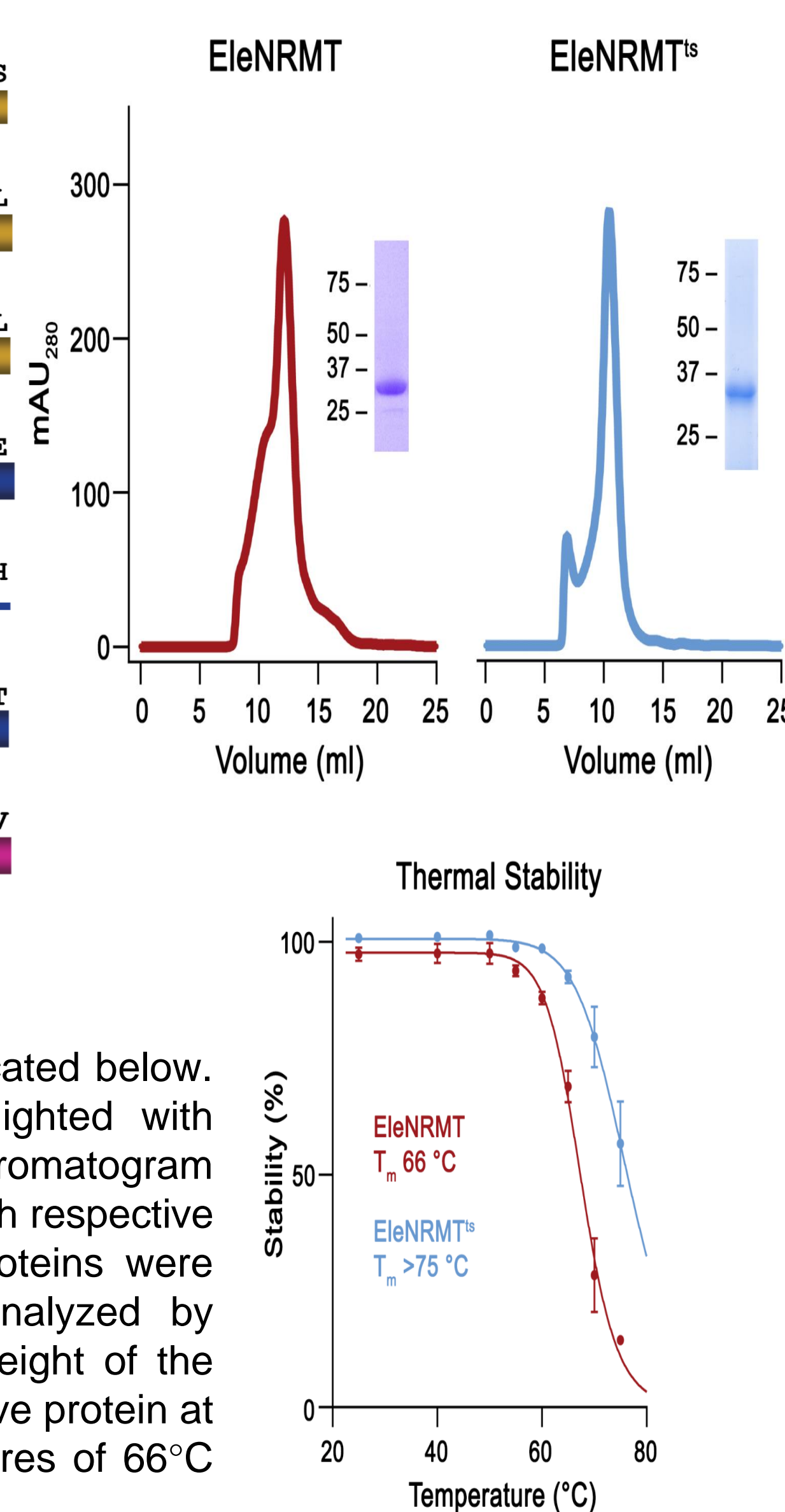
Despite its small size (47 kDa), EleNRMT never crystallized alone. By combining thermostabilisation of EleNRMT by consensus mutagenesis and generation of two nanobodies binding EleNRMT simultaneously, we obtained cryoEM structures in presence and absence of Mg²⁺ at respective resolutions of 3.5Å and 4.1Å. The presence of the two nanobodies allowed the growth of crystals diffracting at 4.1Å. We used the high resolution cryoEM structure as a search model for molecular replacement. The crystals were soaked in a crystallization solution supplemented with Mn²⁺ and its anomalous diffraction properties were used allowing us to identify the substrate binding site. Overall, the structures of EleNRMT revealed a generally similar protein architecture compared to classical NRAMPs, with a restructured ion binding site whose increased volume provides suitable interactions with ions that likely have retained much of their hydration shell. The lack of proton coupling is explained by the absence in EleNRMT of signature proton acceptor residues in standard NRAMPs.

I- Generation of a thermostabilized mutant of EleNRMT

A Thermostabilisation of EleNRMT by consensus mutagenesis



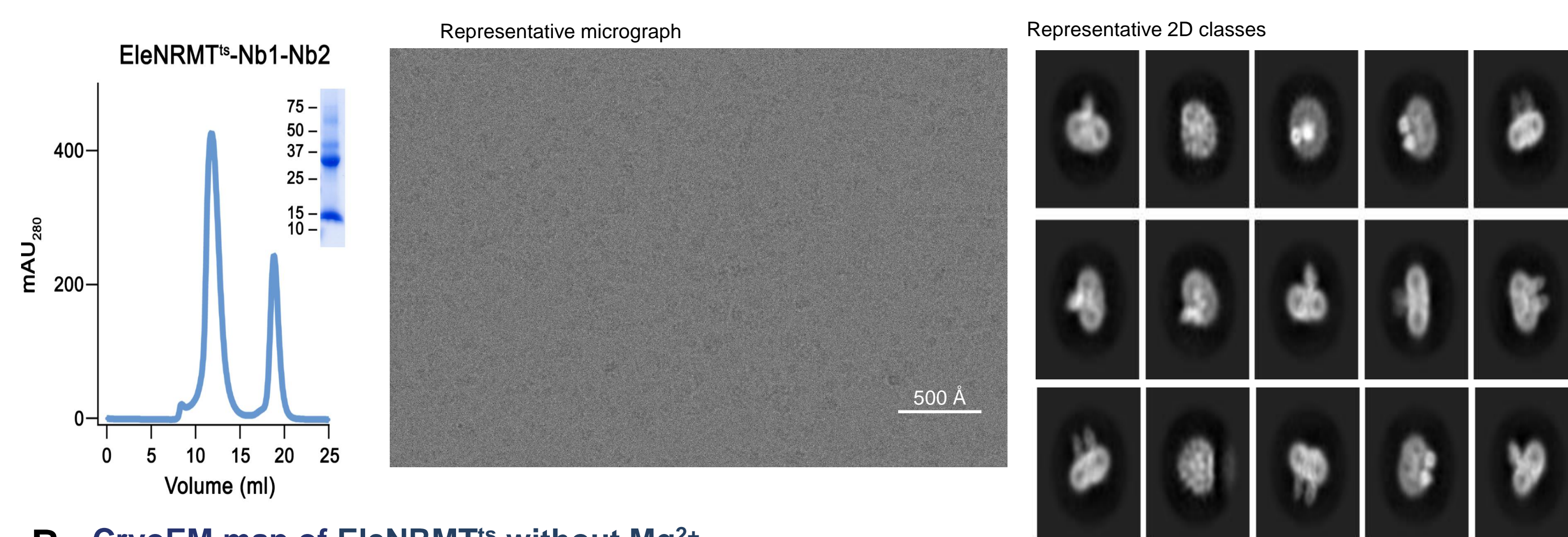
B Biochemical stability of the EleNRMT^{ts} mutant



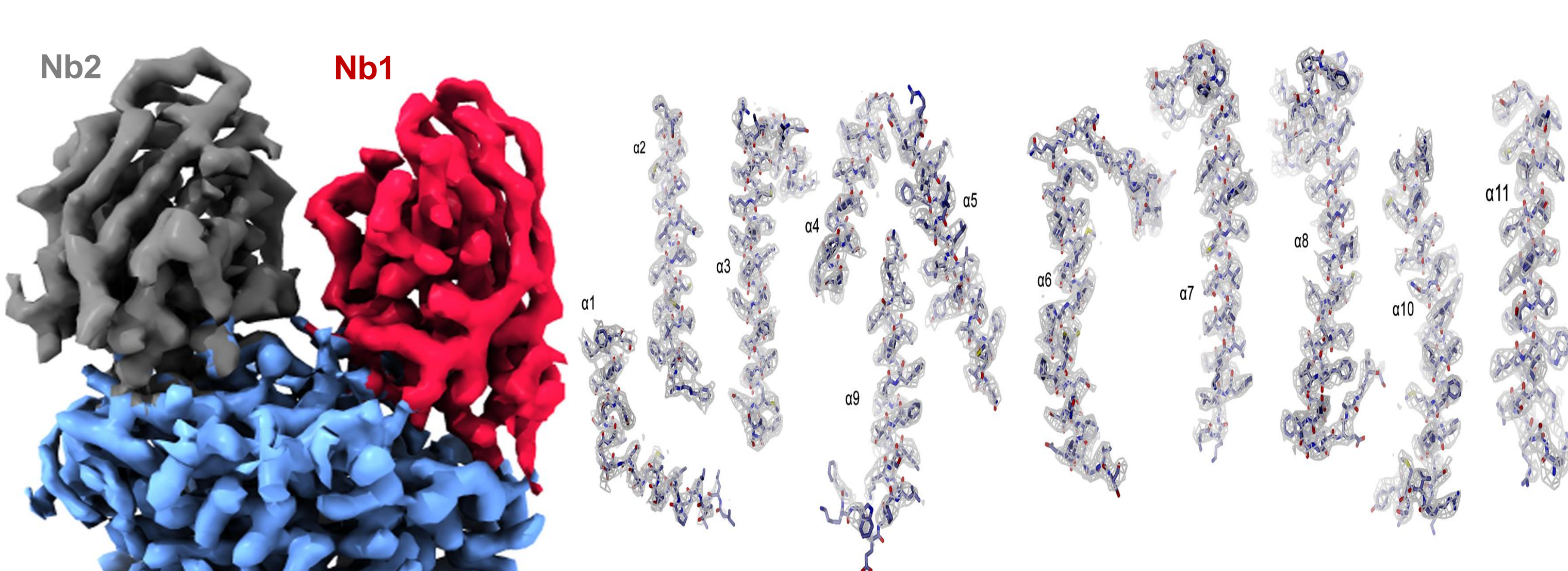
(A) Sequence of EleNRMT with secondary structure elements indicated below. Residues mutated in the thermostabilized EleNRMT^{ts} are highlighted with replacements shown on top. (B) Upper panels: Size exclusion chromatogram after affinity purification of EleNRMT (left) and EleNRMT^{ts} (right) with respective SDS-PAGE gel of the purified protein. Lower panel: Purified proteins were incubated at increasing temperatures. The supernatant was analyzed by fluorescence size exclusion chromatography (FSEC). The peak height of the different samples were normalized to the peak height of the respective protein at 4°C and fitted to sigmoidal equation resulting in melting temperatures of 66°C (EleNRMT) and > 75°C (EleNRMT^{ts}).

II- Structure determination of EleNRMT^{ts} in complex with two nanobodies by CryoEM

A Sample preparation of EleNRMT^{ts} in complex with Nb1 & Nb2



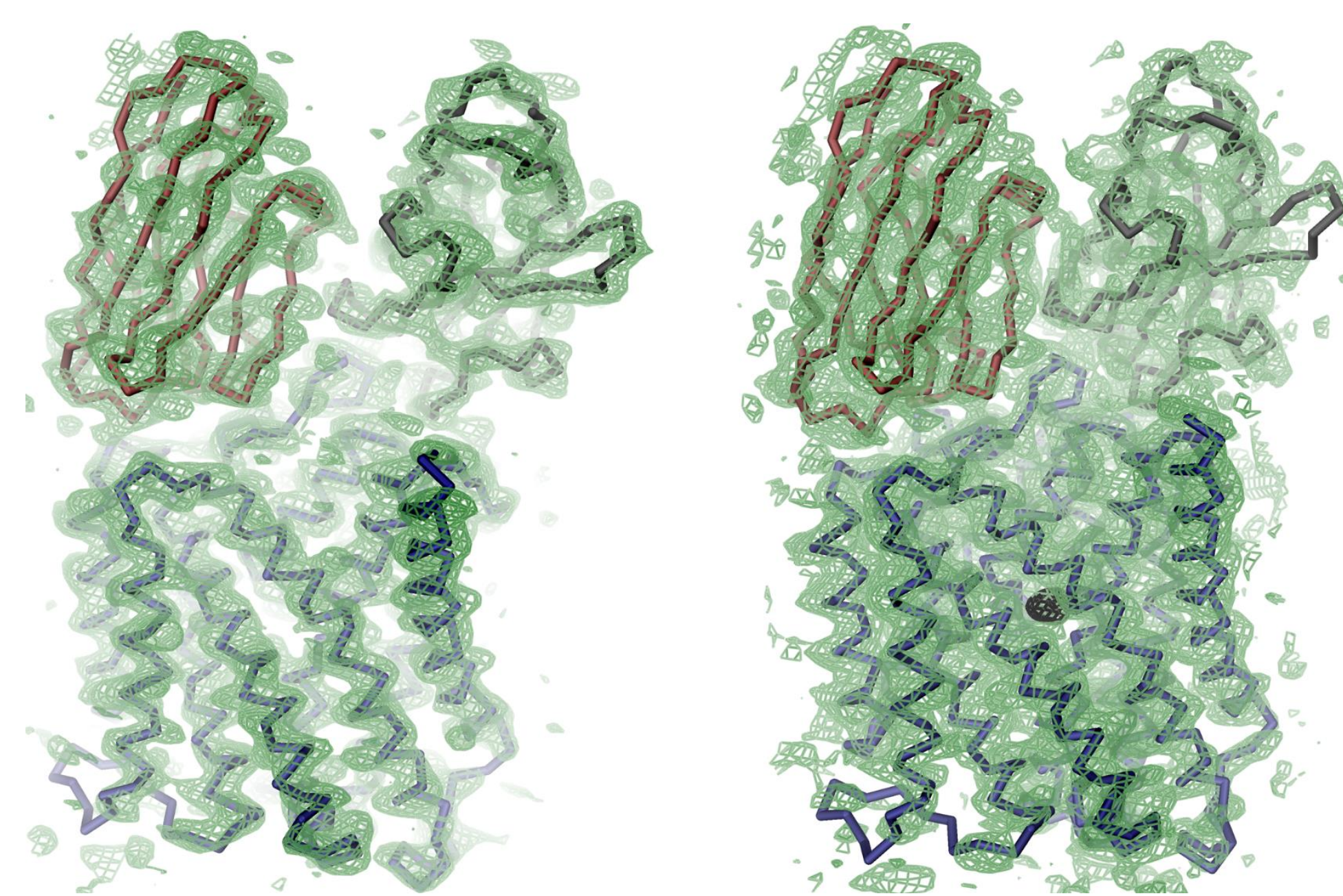
B CryoEM map of EleNRMT^{ts} without Mg²⁺



(A) Left: Size exclusion chromatogram and SDS PAGE gel of purified EleNRMT^{ts} in complex with Nb1 & Nb2 used for structure determination by CryoEM. Middle: Representative micrograph. Right: Representative 2D classes. (B) CryoEM map of EleNRMT^{ts} in complex with Nb1 & Nb2 processed using Cryosparc v3.2. Densities around the 11 helices in EleNRMT^{ts} allows for unambiguous reconstruction.

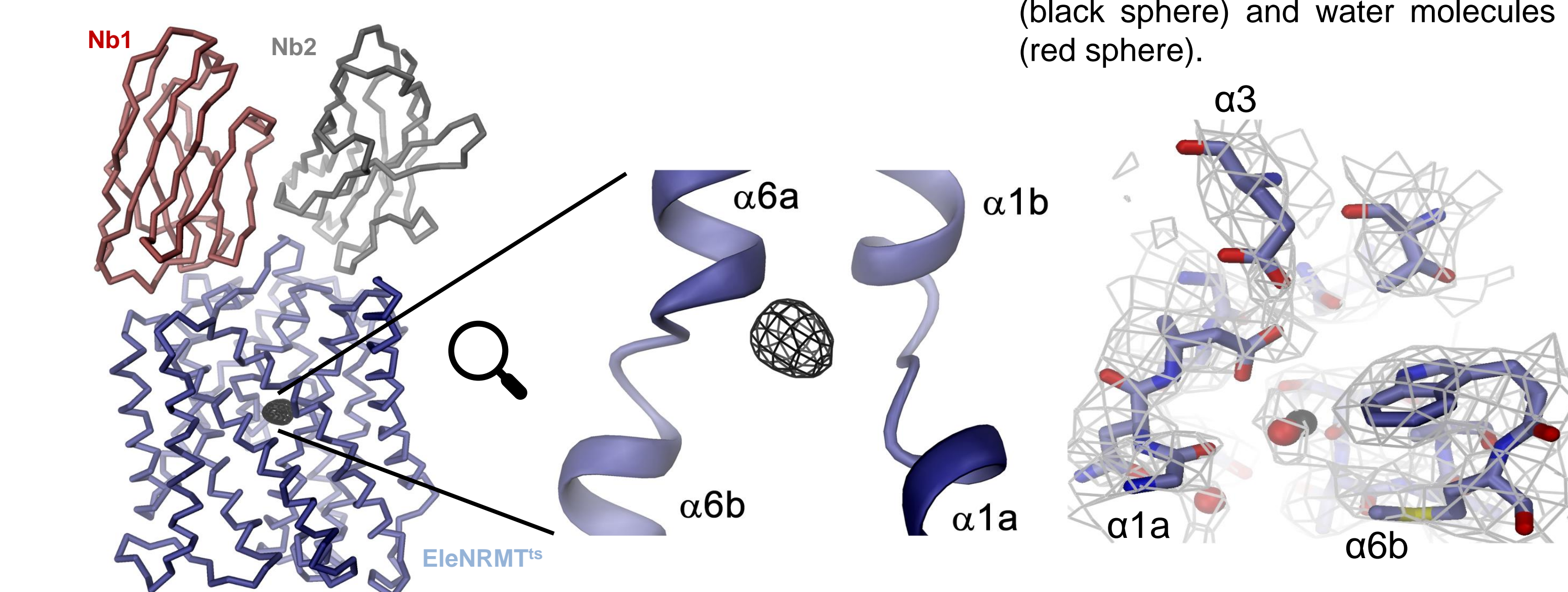
III- Combination of cryoEM and Xray crystallography

A Crystal phasing and soaks in Mn²⁺



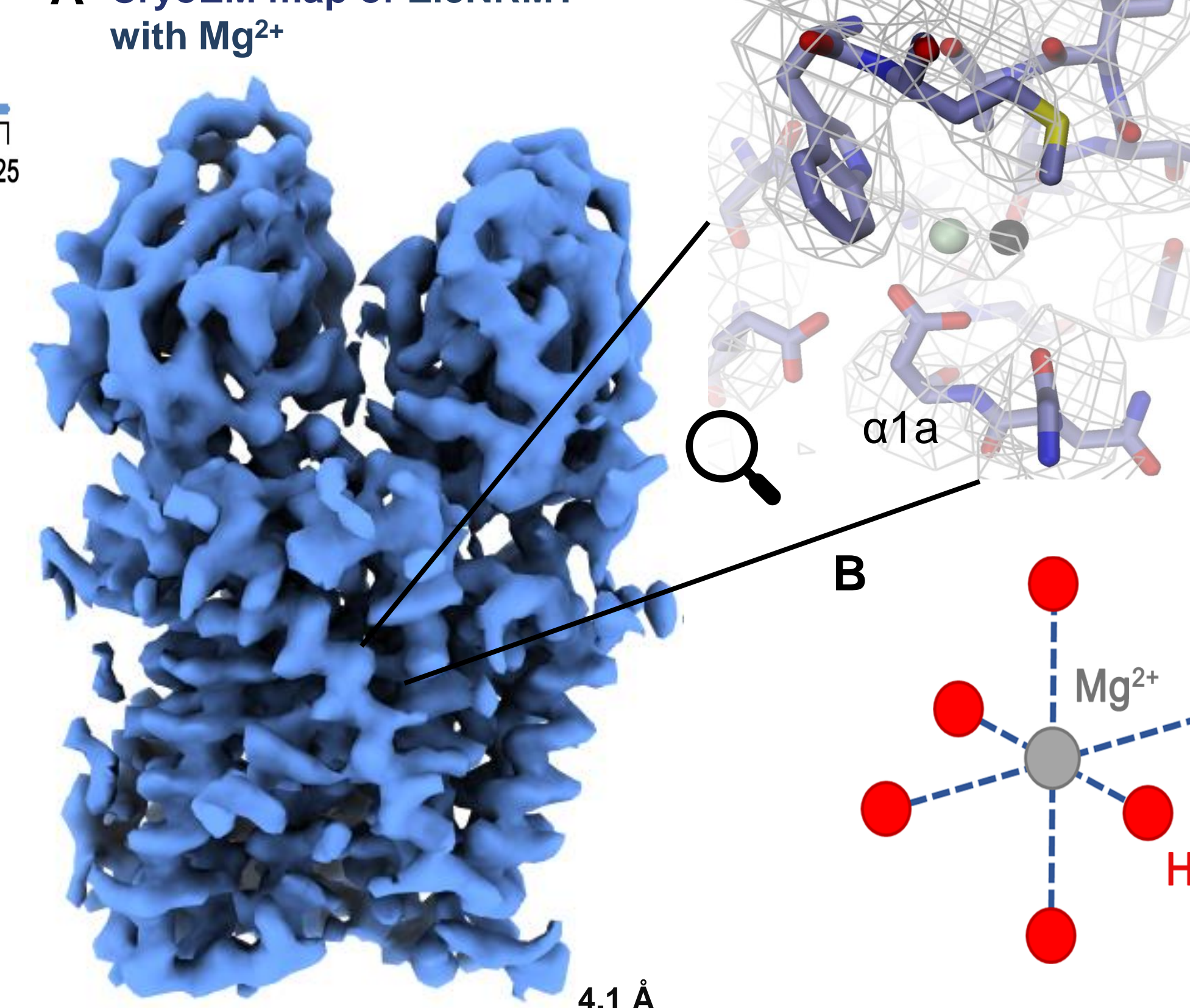
(A) Crystal structures of EleNRMT^{ts}-Nb1-Nb2 complex in absence and presence of Mn²⁺. 2F_o-F_c maps contoured at 1σ. Left: Crystals were phased using the high resolution cryoEM structure and refined leading to a 4.1 Å structure. Right: Crystal structure of the complex soaked in Mn²⁺ at a resolution of 4.6 Å. Anomalous difference electron density was contoured at 4 σ and depicted as black mesh. (B) Left: Superimposition of the cryoEM structure and anomalous difference (black mesh) shows location of the ion binding site. Middle: Zoom on the ion binding site. Right: Residual density in the cryoEM map of apo EleNRMT^{ts}-Nb1-Nb2 complex in vicinity to the Mn²⁺ binding position (black sphere) and water molecules (red sphere).

B Identification of the ion binding site

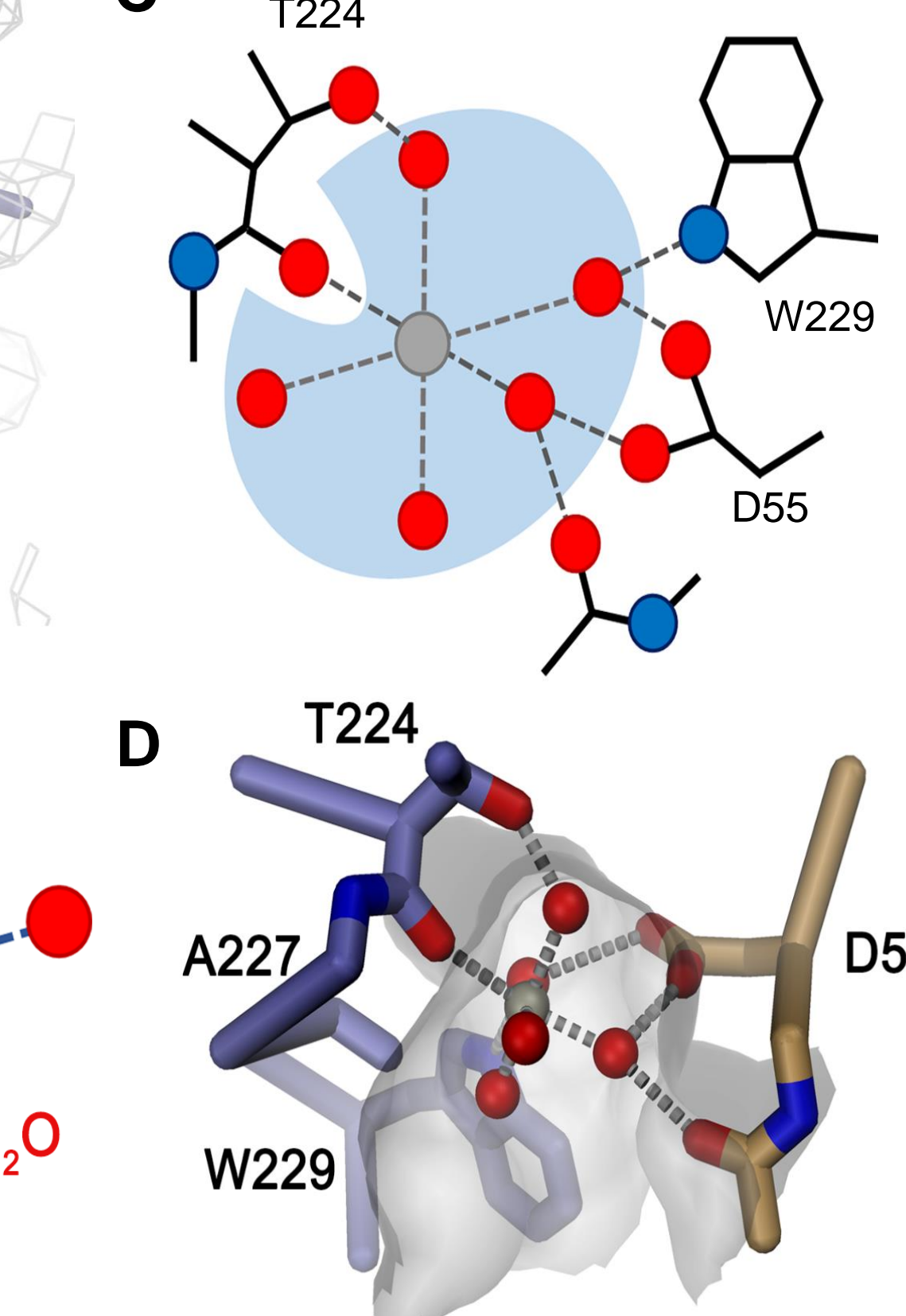


IV- Visualisation of residual density for Mg²⁺ using cryoEM

A CryoEM map of EleNRMT^{ts} with Mg²⁺



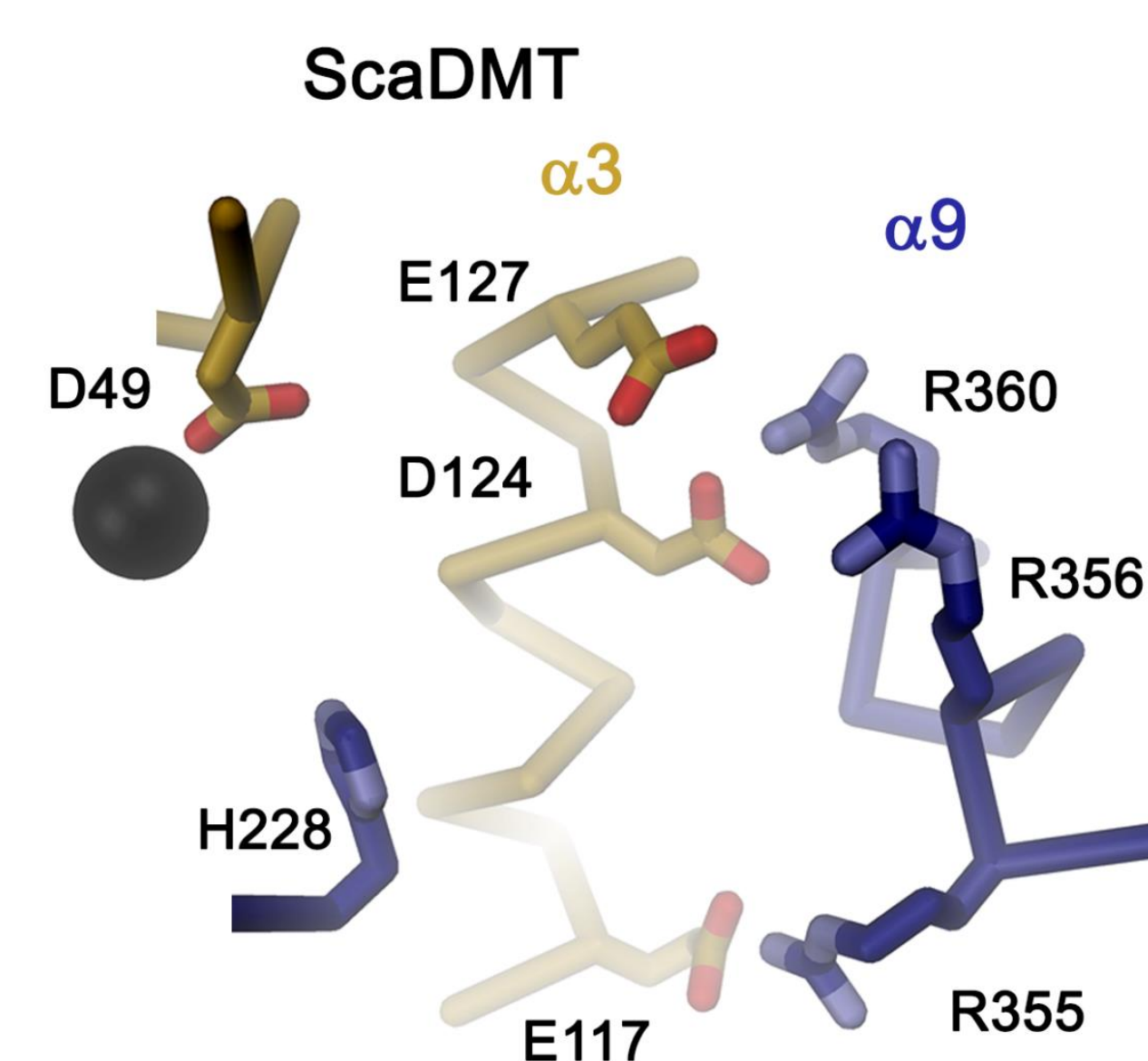
C



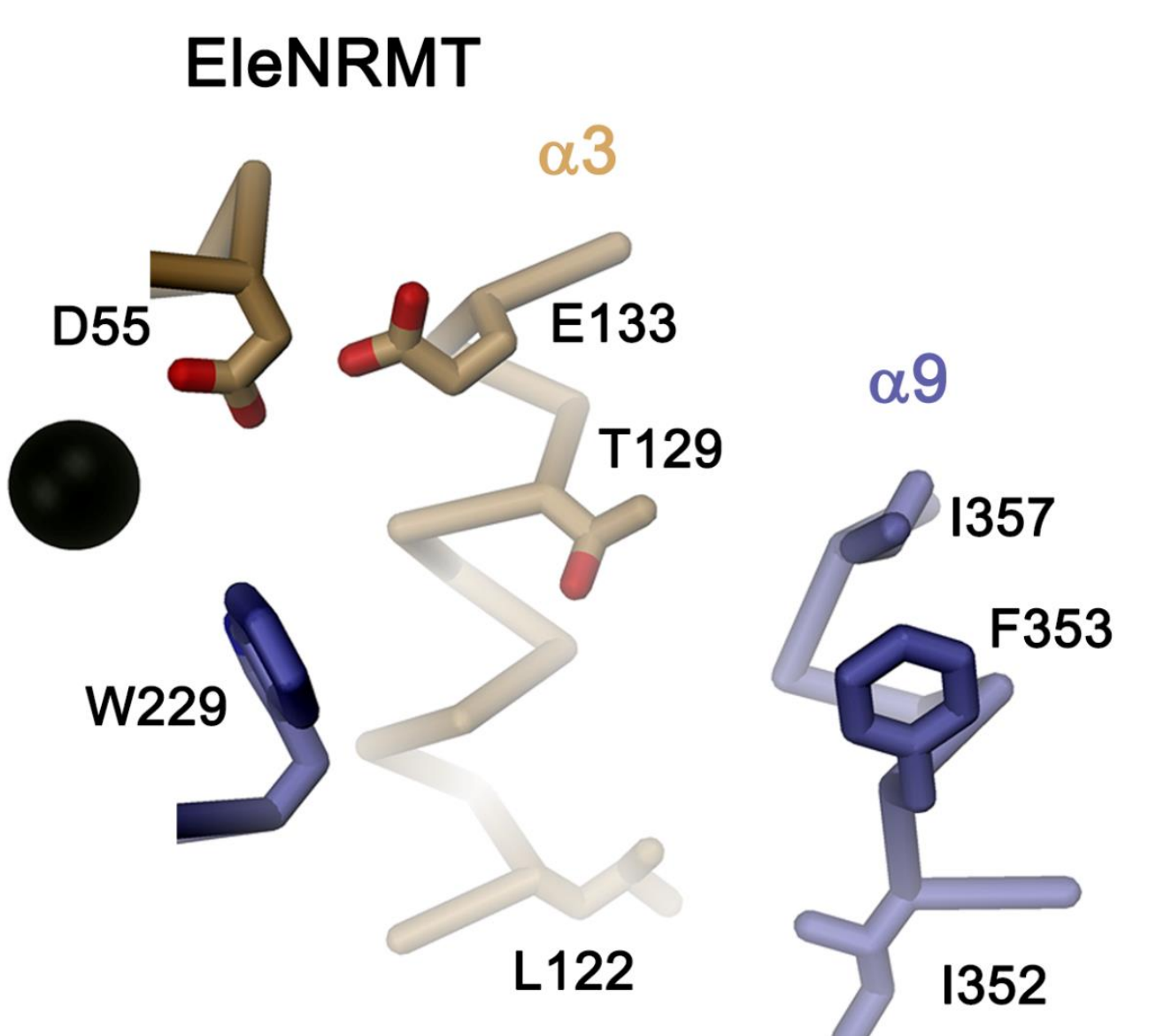
(A) CryoEM map of EleNRMT^{ts} in complex with Nb1 & Nb2 in presence of Mg²⁺. The close up onto the residual density in the ion binding site shows the Mn²⁺ (black sphere) and Mg²⁺ (green sphere) binding position. (B) Schematic depiction of octahedral coordination of the first hydration shell surrounding a Mg²⁺ ion and (C) within the ion binding site of a NRMT. (D) Model of Mg²⁺ bound to the site of EleNRMT. The coordinates of the hydrated Mg²⁺ were obtained from the high-resolution structure of the Mg²⁺ transporter MgtE (PDBID 4U9L).

V- Structures explain absence of proton coupling in EleNRMT

A



B



(A) Region in vicinity of the ion binding site of ScaDMT on α3 and α9 implicated in proton transport in NRAMPs and (B) corresponding region in EleNRMT. Residues involved in proton coupling in ScaDMT include a conserved histidine on α-helix 6b located close to the binding site and an intracellular H⁺ release aqueous pathway made of acidic and basic residues on α-helices 3 and 9. No proton acceptor is present at equivalent positions in EleNRMT.